Published in final edited form as:

Arterioscler Thromb Vasc Biol. 2019 August ; 39(8): 1574–1587. doi:10.1161/ATVBAHA.119.312610.

Hepatic forkhead box protein A3 regulates ApoA-I expression, cholesterol efflux and atherogenesis

Yuanyuan Li[1,*], **Yanyong Xu**[1,*], **Kavita Jadhav**[1], **Yingdong Zhu**[1], **Liya Yin**[1], **Yanqiao Zhang**[1,**]

[1]Department of Integrative Medical Sciences, Northeast Ohio Medical University, Rootstown, OH, USA 44272

Abstract

Objective—To determine the role of hepatic forkhead box A3 (FOXA3) in lipid metabolism and atherosclerosis.

Approach and Results—Hepatic FOXA3 expression was reduced in diabetic or high fat diet-fed mice or patients with nonalcoholic steatohepatitis. We then used adenoviruses to over-express or knock down hepatic FOXA3 expression. Over-expression of FOXA3 in the liver increased hepatic ApoA-I expression, plasma HDL-c level, macrophage cholesterol efflux, and macrophage reverse cholesterol transport. In contrast, knockdown of hepatic FOXA3 expression had opposite effects. We further showed that FOXA3 directly bound to the promoter of the *Apoa1* gene to regulate its transcription. Finally, AAV8-mediated over-expression of human FOXA3 in the hepatocytes of *Apoe*$^{-}$mice raised plasma HDL-c levels and significantly reduced atherosclerotic lesions.

Conclusions—Hepatocyte FOXA3 protects against atherosclerosis by inducing ApoA-I and macrophage reverse cholesterol transport.

Keywords

FOXA3; atherosclerosis; ApoA-I; cholesterol efflux; liver; [90] Lipid and lipoprotein metabolism; [143] Gene regulation; [145] Genetically altered mice

Introduction

Atherosclerosis is the leading cause of deaths in Western countries. Macrophages play a key role in the pathogenesis of atherosclerosis by modulating foam cell formation and inflammatory response. Macrophage reverse cholesterol transport (RCT) is a protective mechanism for atherosclerosis in that it prevents macrophages from accumulation of excessive cholesterol. In the early stage of macrophage RCT, ATP binding cassette subfamily A member 1 (ABCA1) effluxes free cholesterol and phospholipids to lipid free ApoA-I to form preβ-HDL. Preβ-HDL accepts more free cholesterol from peripheral tissues to become spherical α-HDL particles after free cholesterol is esterified to form cholesteryl

Address correspondence to: Yanqiao Zhang, MD, Northeast Ohio Medical University, 4209 State Route 44, Rootstown, Ohio 44272, Tel. 330-325-6693, Fax. 330-325-5910, yzhang@neomed.edu.

*Contributed equally to this work.

c) **Disclosures:** None.

esters (CE) by lethicin:cholesterol acyltransferase (LCAT). Mature HDL is up-taken by the liver via scavenger receptor group B type 1 (SR-BI). In humans, HDL-C may be transferred to ApoB-containing lipoproteins by cholesterol ester transfer protein (CETP) and subsequently return to the liver via LDL receptor (LDLR)-mediated endocytosis [1].

ApoA-I is the most abundant apolipoprotein of HDL. For many years, plasma HDL level has been known to be inversely associated with the risk of CVD [2]. However, recent studies have demonstrated that HDL functionality, not the HDL level *per se*, is more relevant to atheroprotection [2–4]. Transgenic over-expression of human ApoA-I raises plasma HDL-C levels and protects against atherosclerosis [5–7]. An increase in plasma ApoA-I levels through intravenous (i.v.) infusion of ApoA-I mimetics or hepatic overexpression of ApoA-I also promotes macrophage RCT and prevents or regresses atherosclerosis [8, 9]. In contrast, ApoA-I deficiency impairs macrophage RCT and promotes atherogenesis [10]. In addition, supplement of ApoA-I or ApoA-I mimetics to hypercholesterolemic mice also reduces recruitment of immune cells to the plaque [11–13], which may also contribute to the athero-protective effect of ApoA-I. In addition to ApoA-I, ApoM is also required for preβ-HDL formation and protects against atherosclerosis in *Ldlr*$^{-/-}$ mice [14].

The major function of HDL is to promote RCT. In addition, HDL is known to have anti-oxidant and anti-inflammatory properties [15]. Paraoxonase 1 (PON1) is an HDL-associated antioxidant enzyme that is mainly synthesized in the liver. PON1 is responsible for many of HDL's athero-protective properties, such as HDL-mediated cholesterol efflux from macrophages and inhibition of LDL oxidation [16]. Gain- and loss-of-function studies have demonstrated that PON1 protects against atherosclerosis in mice [16].

Systemic inflammation may alter HDL's functionality by modulating the content of serum amyloid A (SAA) or other mediators in HDL [17]. SAAs are acute-phase proteins. Plasma SAA proteins are mainly produced by the liver and are associated with HDL. SAA can induce adhesion molecules in vascular walls, such as intracellular adhesion molecule 1 (ICAM-1), vascular cell adhesion molecule 1 (VCAM-1), E-selectins, etc [18]. SAA1 and SAA2 are shown to promote early atherogenesis by impairing HDL's ability to promote cholesterol efflux and HDL's anti-inflammatory properties [19]. Other lines of data indicate that oxidized lipids in HDL can promote monocyte adhesion to endothelium [20], a key early step in atherogenesis.

Forkhead box A3 (FOXA3) is a member of the winged-helix transcription factors and is expressed in the liver, adipose tissue, intestine, pancreas, testis, etc. FOXA3 regulates gene expression mainly by binding to the consensus sequences TGTTTAC in the target genes [21]. FOXA3 may also serve as a pioneer transcription factor by maintaining an accessible nucleosome configuration at enhancers for tissue specific gene activation [22]. Several studies have shown that co-transfection of FOXA3 together with other hepatocyte factors can convert fibroblasts to hepatocyte-like cells [23–25] or hepatic stem cells [26], suggesting a key role of FOXA3 in liver development. In testis, *Foxa3* ablation leads to loss of germ cells [27, 28], indicating that FOXA3 is important in germ cell maintenance.

FOXA3 may also play a role in glucose homeostasis. In vitro studies suggest that FOXA3 activates the gene transcription of phosphoenolpyruvate carboxykinase (*Pepck*) and glucose-6-phosphatase (*G6pase*) [29, 30], two important gluconeogenic genes. Interestingly, *Foxa3*$^{-/-}$ mice show reduced plasma glucose levels after a 24–72 h fast, but hepatic *Pepck* or *G6pase* expression is not reduced [31]. In contrast, hepatic glucose transporter 2 (*Glut2*) is markedly reduced in *Foxa3*$^{-/-}$ mice [31], which may account, at least in part, for the hypoglycemic phenotype in these mice during a prolonged fast.

The role of FOXA3 in adipose tissue has been relatively well established. FOXA3 is up-regulated in adipose tissue by activation of the glucocorticoid receptor signaling [32] and during aging [33]. FOXA3 promotes adipocyte differentiation by inducing peroxisome proliferator-activated receptor gamma (PPARγ) [34]. Consistent with this finding, mid-age *Foxa3*$^{-/-}$ mice have increased white fat browning, thermogenic capacity and longevity, and reduced adipose tissue expansion [33]. Moreover, genetic ablation of *Foxa3* also reduces high fat diet-induced epididymal fat depot [34] and protects mice from long-term effects of dexamethasone treatment on fat accretion [32].

So far, the role of FOXA3 in regulating lipoprotein metabolism or atherosclerosis is completely unknown. In this study, we used gain- and loss-of-function approaches to show that hepatic FOXA3 is a key regulator of ApoA-I expression and macrophage RCT. As a result, AAV8-mediated over-expression of human FOXA3 protects against atherosclerosis in *Apoe*$^{-/-}$ mice.

Materials and Methods

The authors declare that all supporting data are available within the article or in the online-only Data Supplement or from the corresponding author on request.

Human liver tissues, mice and diets

C57BL/6J mice, *ob/ob* mice, *db/db* mice, lean mice and *Apoe*$^{-/-}$ mice were purchased from the Jackson Laboratories (Bar Harbor, Maine, USA). The high fat diet (HFD) containing 60% kcal from fat was purchased from Research Diets (D12492), and the high fat/high cholesterol diet (Western diet) containing 42% fat/0.2% cholesterol was purchased from Envigo (TD.88137). Mice were fed an HFD or HFHC diet for 12–20 weeks (see figure legends). In general, male mice were used and fasted for 5–6 h prior to euthanization unless otherwise stated. Human liver samples were obtained from the Liver Tissue Cell Distribution System at University of Minnesota and have been described previously [35]. All the animal experiments were approved by the Institutional Animal Care and Use Committee at Northeast Ohio Medical University (NEOMED). The use of human tissue samples was approved by the Institutional Review Board at NEOMED.

Adeno-associated viruses (AAVs) and adenoviruses

Human FOXA3 coding sequence was cloned into an AAV vector under the control of a mouse albumin promoter (AAV-ALB-hFOXA3). AAV8-ALB-hFOXA3 or AAV8-ALB-null (control) was produced and titrated by Vector BioLabs. Each mouse was i.v. injected with 3×10^{11} genome copies (GC) of AAV and then fed an HFCF diet for 3 months. Adenoviruses

expressing human FOXA3 as well as Flag and His tags at the C terminal were purchased from ViGene Biosciences (Cat # VH813611). Adenoviruses expressing an shRNA against *Foxa3* were generated using a BLOCK-IT™ U6 RNAi Entry Vector Kit (Thermo Fisher). The targeting sequence was CCCTGAGTGAAATCTACCAAT. Adenoviruses were amplified in 293A cells, purified with cesium chloride, and titrated using the Adeno-X™ Rapid Titer Kit (Clontech).

qRT-PCR

RNA was extracted using Trizol Reagent (Thermo Fisher) and mRNA levels were analyzed by quantitative real-time PCR (qRT-PCR) using SYBR Green (GeneCopoeia) on a 7500 Real Time PCR machine (Applied Biosystems). mRNA levels were normalized to 36B4.

Western blot assays

Western blot assays were performed using whole liver lysates, nuclear extracts, or plasma lipoprotein fractions separated by fast protein liquid chromatography (FPLC) as described previously [36–38]. FOXA3 antibody was purchased from Santa Cruz (Cat # SC-5361). PON1 and tubulin antibodies were purchased from Abcam (Cat # ab126597 and ab4074, respectively). ApoA-I antibody was purchased from Meridian Life Sciences (Cat # K23001R). SAA1 antibody was purchased from R & D Systems (Cat # AF2948). SREBP1 (Cat # NB600–582) and beta-actin (Cat # NB600–501) antibodies were purchased from Novus. CD36 antibody was purchased from Thermo Fisher (Cat # PA116813). Histone antibody was purchased from Cell Signaling (Cat # 9671). All the Western blot assays have been repeated once.

Mouse primary hepatocytes and MTT (3-(4,5-dimethythiazol-2-yl)-2,5-diphenyl tetrazolium bromide) assays

Mouse primary hepatocytes were isolated and cultured in DMEM with 10% FBS as described previously [39, 40]. They were infected with adenoviruses. After 48 h, RNA was isolated for qRT-PCR. Some primary hepatocytes were treated with 100–500 μM palmitate or oleate. To prepare the 5 mM palmitate or oleate stock, palmitate or oleic acid was mixed with BSA at a ratio of 3:1. The stock solutions were then diluted into prewarmed culture medium without fetal bovine serum (FBS) to achieve a final solution of 100–500 μM. The control group was treated with the same concentration of BSA. Cell proliferation/viability assays were performed using an MTT Assay Kit (Abcam, cat # ab211091).

Ki-67 immunostaining

Paraffin-embedded liver sections were immunostained using a Vectastain Elite ABC-HRP kit (Cat # PK-6104. Vector Laboratories) and a Ki-67 antibody (ThermoFisher, Cat # MA5–14520).

Luciferase reporter assays

The mouse *Apoa1* gene promoter with different lengths (- 1.8 kb, −1.0 kb or - 0.5 kb to +100 bp) was amplified by PCR and cloned into the pGL3-luciferase reporter vector (Promega). The two putative FOXA3 binding sites TCCTGTTTGCC (site 1) and

CTCTGTTTGCC (site 2) were mutated to TCCgcgggGCC (site 1) and CTCgcgggGCC (site 2), respectively using the QuikChange II Site-Directed Mutagenesis Kit (Agilent). All PCR-generated constructs and mutants were confirmed by DNA sequencing. Luciferase activity was measured as described previously [39]. In brief, HepG2 cells were transfected with pGL3-luciferase reporter plasmids together with pCMV-β-gal, pCMV-FOXA3 or pCMV6 (control) using Lipofectamine 2000 (Life Technologies). After 36 h, luciferase activity was analyzed using the Luciferase Reporter Assay System Kit (Promega) and normalized to β-gal activity. β-gal activity was measured using ONPG as substrate.

Electrophoretic mobility shift assay (EMSA)

50 base pair of oligonucleotides containing 2 putative Foxa3 binding sites were synthesized and labeled by biotin on the 3′ end following the manufacturer's instruction (Cat # 89818, Thermo Fisher Scientific). EMSA was performed using a kit according to the manufacturer's instructions (Cat # 20148, Thermo Fisher Scientific). 293A cell lysate overexpressing FOXA3 was used for incubation with probes. Competition studies were performed by adding unlabled oligonucleotides, including WT oligo (oligo containing putative Foxa3 binding sites), mut1 oligo (oligo with site 1 mutation), mut2 oligo (oligo with site 2 mutation), or mut½ oligo (oligo with site 1 and site 2 mutations). For the supershift assay, 293A cell lysates were incubated with the probe first, followed by incubation with an FOXA3 antibody. Same amount of IgG was used as the negative control. We have repeated EMSA once.

Chromatin immunoprecipitation (ChIP) assay

Livers of mice infected with Ad-Empty or Ad-FOXA3 were homogenized in cold 1xPBS containing the protease inhibitor cocktail (Roche, NJ), 2 μg/ml PMSF, 1 mM EDTA and 1 mM EGTA. Chromatin immunoprecipitation was carried out using a ChIP assay kit (Cat # 17–295; Millipore, MA) according to the manufacturer's protocol with minor modifications. Briefly, the liver homogenate was filtered to remove debris and then crosslinked with 1% formaldehyde. After sonication and preclearance with Protein A beads, sheared chromatin was then immunoprecipitated using a goat IgG or anti-FOXA3 antibody (Santa Cruz Biotechnology). After elution, the precipitated DNA/antibody complex was digested with proteinase K. DNA was then extracted and used for qPCR analysis with primers flanking the two putative FOXA3-binding sites in the *Apoa1* promoter. The supernatant before immunoprecipitation of each sample was used as its own input control.

Analysis of plasma lipids, cortisol and testosterone levels

Plasma triglyceride or cholesterol levels were determined using Infinity regents (Thermo Fisher). HDL or VLDL/LDL cholesterol was measured using an HDL and LDL/VLDL quantification kit (Cat # K613, Biovision Inc). Plasma cortisol (Cat # 500360) and testosterone (Cat # 582701) levels were measured using ELISA kits from Cayman.

Pulse-chase studies

Pulse-chase studies were performed as described previously [41]. Briefly, primary hepatocytes were infected with Ad-Empty or Ad-Foxa3 (MOI=10) for 36 h, and then washed with

1xPBS prior to incubation for 1 hour with leucine and FBS-free DMEM. The hepatocytes were then incubated/pulsed with [^{3}H]-leucine (200 μCi/mL; Cat # NET116600, PerkinElmer) for 2 hours. After pulsing, cells were washed 4 times with 1xPBS and placed in chase medium (leucine- and FBS-free DMEM, with 15 μg/mL of cycloheximide (Cat # 239764, Sigma)) for 2 hours. Culture medium and cell lysates were collected for ApoA-I immunoprecipitation using an ApoA-I antibody (Cat # K23001R, Meridian) and protein A agarose/salmon sperm DNA (Cat # 16–157, Millipore) and analyzed by 12% SDS-PAGE. Purified ApoA-I protein standard (2 μg/lane; Cat # SRP4693, Sigma) was mixed with each sample before electrophoresis for visual identification of ApoA-I bands. The gels were stained with Coomassie blue, and the bands corresponding to ApoA-I were excised and counted using a liquid scintillation counter.

Fast protein liquid chromatography (FPLC) assay

Plasma lipoprotein profile was analyzed by FPLC as described [42]. Briefly, after 100 μl plasma was injected, lipoproteins were run at 0.5 ml/min in a buffer containing 0.15 M NaCl, 0.01 M Na_2HPO4, 0.1 mM EDTA, pH 7.5, and separated on a Superose 6 10/300 GL column (GE Healthcare) by using BioLogic DuoFlow QuadTec 10 System (Bio-Rad, CA). 500 μl of sample per fraction was collected. Triglyceride or cholesterol levels in each fraction were determined using Infinity reagents (Thermo Fisher).

Cholesterol efflux assay

Mouse serum was depleted of ApoB-containing lipoprotein by using PEG-6000 (Cat # CAS 25322–68-3, Sigma-Aldrich). Peritoneal macrophages were seeded in a 24-well plate and loaded with 0.5 μCi/ml [^{3}H]cholesterol (PerkinElmer) for 24 h. After extensive wash with 1xPBS, cells were incubated in DMEM supplemented with 0.2% fatty acid–free BSA for 4 h. The cells were washed again by PBS and then incubated in fresh DMEM containing 0.2% BSA in the presence of 2.8% ApoB-depleted serum. Supernatants were collected after 4 h and the level of [^{3}H]cholesterol was quantified by scintillation counting. Values are expressed as a percentage of total cell [^{3}H]cholesterol content (effluxed [^{3}H]cholesterol + cell-associated [^{3}H]cholesterol).

Reverse cholesterol transport

Reverse cholesterol transport (RCT) was performed as described previously [43, 44]. In brief, peritoneal macrophages were isolated and incubated for 48 h in DMEM containing 10% FBS, 5 μCi/ml [^{3}H]cholesterol and 25 μg/ml Ac-LDL, followed by wash in PBS and equilibration for 4 h in DMEM supplemented with 0.2% BSA and penicillin/streptomycin. Before injection, cells were pelleted and re-suspended in serum-free DMEM. 0.5 ml of macrophages (~ 5×10^6 cells) containing ~ $6.5–10\times10^6$ counts per minute (cpm) were injected intraperitoneally into C57BL/6 mice infected with adenoviruses. Blood and feces were collected at 48 h. Plasma, hepatic and fecal ^{3}H-tracers were assayed using a liquid scintillation counter and values are expressed as a percentage of total injected radioactivity.

Atherosclerosis study

This experiment adhered to the guidelines for experimental atherosclerosis studies described in the American Heart Association Statement [45]. We used male mice in this study because estrogen is known to affect the outcome of atherosclerotic studies [46]. The aorta, including the ascending arch, thoracic, and abdominal segments, and aortic root were isolated and gently cleaned of the adventitia. Aortic root was dissected and embedded in optimal cutting temperature compound, and then frozen on dry ice. Serial 7-mm-thick cryosections from the middle portion of the ventricle to the aortic arch were collected on superfrost plus microscope slides (Cat # 12–550-15, Fisher Scientific). In the region beginning at the aortic valves, every other section was collected. Sectioned aortic roots or *en face* aortas were stained with oil red O and the atherosclerotic plaque size determined using the Image-Pro software (Media Cybernetics) as described previously [47]. Immunostaining of aortic roots with a MOMA-2 antibody (Bio-Rad, Cat # MCA 519G) was conducted using a Vectastain Elite ABC-HRP kit (Cat # PK-6104. Vector Laboratories).

Statistical analysis

We used GraphPad Prism 8.1.1 (GraphPad, CA) for statistical analysis. Normality and equal variances tests were performed. If data passed both tests, we used unpaired Student *t* test followed by Welch's corrections. If the sample did not pass normality or equal variance test, statistical analyses were performed using unpaired Mann-Whitney *U* test. All values are expressed as mean±SEM. Differences were considered statistically significant at $P<0.05$.

Results

Hepatic FOXA3 expression is reduced in HFD-fed or diabetic mice and NASH patients

So far, little has been known about the role of hepatic FOXA3 in metabolic regulation. We first investigated whether nutritional or disease statuses affected hepatic FOXA3 expression. In C57BL/6J mice, high fat diet (HFD) feeding reduced hepatic *Foxa3* mRNA and protein expression by >50% but induced cluster differentiation factor 36 (*Cd36*) by >3 fold (Fig. 1A–C). HFD is known to induce CD36 [48]. In diabetic and obese *ob*/*ob* mice (Fig. 1D–F) or *db*/*db* mice (Fig. 1G–I), hepatic *Foxa3* mRNA and protein levels were also reduced by >50% whereas sterol regulatory element-binding protein 1 (SREBP1) was induced by >2 fold. In NASH patients, we also observed a >50% reduction in hepatic *FOXA3* mRNA and protein levels (Fig. 1J–L).

In an attempt to understand the mechanism leading to reduced hepatic FOXA3 expression, we treated primary hepatocytes with either palmitate or oleic acid, two of the most abundant fatty acids in the liver. Treatment of primary hepatocytes with 100–300 μM palmitate or oleic acid did not affect cell viability (Supplementary Fig. IA **and** IB). When primary hepatocytes were treated with 250 μM palmitate or oleic acid, *Foxa3* protein expression was reduced by >50% (Supplementary Fig. IC–E). Since hepatic free fatty acid (FFA) levels are known to be increased in obesity, diabetes and NAFLD [49–52], the elevated FFAs may contribute to the reduction in hepatic FOXA3 expression in diabetic or HFD-fed mice or NASH patients.

Hepatic over-expression of FOXA3 increases plasma ApoA-I and HDL-c levels

The finding that hepatic FOXA3 is reduced by >50% under metabolic stress led us to determine whether hepatic FOXA3 regulates lipid metabolism. Adenovirus-mediated over-expression of human FOXA3 (Ad-hFOXA3) in the livers of C57BL/6 mice increased plasma HDL-c levels by 150% without affecting plasma VLDL/LDL-c levels (Fig. 2A). Over-expression of human FOXA3 by Ad-hFOXA3 had no effect on plasma levels of ALT, AST, cortisol, testosterone or glucose (Supplementary Fig. IIA–D) or hepatic cholesterol levels (Supplementary Fig. IIE). In the liver, human FOXA3 over-expression significantly induced several genes involved in HDL biogenesis (*Abca1*, *Apoa1*, *Apoa2*, *Apom* and *Lcat*), inflammation (*Pon1*) or lipoprotein uptake (*Apoe*) (Fig. 2B). FOXA3 also repressed acute phase genes *Saa1*, *Saa2* and *Saa3* but had no effect on the mRNA levels of *Ldlr* or *Scarb1* (*SR-BI)* (Fig. 2B). Consistent with the change in mRNA levels, hepatic ApoA-I and PON1 protein levels were increased by >2 fold (Fig. 2C and 2D).

Analysis of plasma lipoprotein profile by fast protein liquid chromatography (FPLC) showed that over-expression of FOXA3 raised plasma HDL-c levels (Fig. 2E), which is consistent with the data of Fig. 2A. In addition, FOXA3 increased ApoA-I and PON1 protein levels but reduced SAA1 protein levels in HDL fractions (Fig. 2F). Thus, hepatic FOXA3 may regulate HDL biogenesis.

In line with previous reports showing that FOXA3 regulates PEPCK and Glut2 gene transcription [29–31], FOXA3 over-expression induced *Pepck* and *Glut2* mRNA levels and tended to increase *G6pase* mRNA levels (Supplementary Fig. IIF). Interestingly, FOXA3 over-expression did not change plasma glucose levels (Supplementary Fig. IID**)**, suggesting that hepatic FOXA3 may also regulate other pathways to counter its effect on gluconeogenesis. In addition, FOXA3 also induced *Foxo1* and *Foxo4* expression (Supplementary Fig. IIF), but the role of such a regulation remains to be investigated.

The cytochrome P450 enzymes are largely expressed in adult differentiated hepatocytes, and play an important role in detoxification/bioactivation of xenobiotics. FOXA3 over-expression is shown to induce CYP2C genes in HepG2 cells [53]. So far, it is unclear whether FOXA3 also regulates mouse *Cyp2c* genes. The data of Supplementary Fig. IIG show that FOXA3 up-regulated *Cyp2c-67*, *Cyp2c-68* and *Cyp2c-70*, but repressed *Cyp2c-38*, *Cyp2c-39*, *Cyp2c-65* and *Cyp2c-66*. The significance of such regulations remains to be explored.

Knockdown of hepatic FOXA3 reduces plasma ApoA-I and HDL-c levels

To investigate whether reduced FOXA3 expression in the liver has opposite effects, we generated an adenovirus expressing shRNA against *Foxa3* (Ad-shFoxa3). Knockdown of hepatic *Foxa3* reduced plasma HDL-c by 46% without affecting plasma VLDL/LDL-c levels (Fig. 3A). Knockdown of hepatic *Foxa3* also raised plasma ALT and AST levels (Fig. 3B). Analysis of hepatic gene expression showed that *Foxa3* deficiency reduced the mRNA levels of *Apoe*, *Apoa1*, *Apoa2*, *Apom* and *Pon1* but induced interleukin 6 (*Il6*), tumor necrosis factor α (*Tnfα*), *Saa1*, *Saa2* and *Saa3* (Fig. 3C and 3D). Over-expression of *Foxa3* shRNA also reduced hepatic FOXA3 and ApoA-I protein levels by 83% and 47%, respectively (Fig.

3E and 3F). FPLC analysis of plasma lipoprotein profile showed that hepatic *Foxa3* deficiency reduced plasma HDL-c level (Fig. 3G). In addition, hepatic *Foxa3* deficiency reduced plasma ApoA-I protein levels but induced SAA1 protein levels by 1.5 to 1.7 fold in HDL fractions 28–30 (Fig. 3H). These loss-of-function data are consistent with our findings collected from mice over-expressing hepatic FOXA3 (see Fig. 2).

Hepatic *Foxa3* deficiency had no effect on plasma cortisol, testosterone or glucose levels or hepatic cholesterol levels (Supplementary Fig. IIIA–D). In the liver, loss of hepatic *Foxa3* had no effect on *Foxa1* or *Foxa2* mRNA levels (Supplementary Fig. IIIE), but reduced the mRNA levels of *Glut2*, *Foxo4*, *Cyp2c-37*, *Cyp2c-67*, *Cyp2c-68* and *Cyp2c-69*, and induced the mRNA levels of *Foxo3*, *Cyp2c-38*, *Cyp2c-39*, *Cyp2c-65* and *Cyp2c-66* (Supplementary Fig. IIIF **and** IIIG). These data are largely consistent with those collected from mice over-expressing hepatic FOXA3 (see Supplementary Fig. II).

Hepatic FOXA3 regulates macrophage cholesterol efflux and reverse cholesterol transport

Over-expression of hepatic ApoA-I induces macrophage RCT and reduces the development of atherosclerosis [8, 54]. In contrast, loss of ApoA-I inhibits macrophage RCT and increases the development of atherosclerosis [10, 55]. The data of Figs. 2 and 3 indicate hepatic FOXA3 is an important regulator of hepatic and plasma ApoA-I expression, suggesting that hepatic FOXA3 may regulate macrophage RCT and/or atherogenesis. Using plasma isolated from mice over-expressing or lacking hepatic *Foxa3*, we showed that over-expression of hepatic *FOXA3* induced macrophage cholesterol efflux (Fig. 4A) whereas hepatic *Foxa3* deficiency had an opposite effect (Fig. 4B). Consistent with these data, over-expression of hepatic *FOXA3* increased [^{3}H]tracers in the plasma (Fig. 4C), liver (Fig. 4D) and feces (Fig. 4E) in mice that were i.p. injected with macrophages loaded with [^{3}H]cholesterol. In contrast, in mice deficient in hepatic *Foxa3*, [^{3}H]tracers were reduced in the plasma (Fig. 4F), unchanged in the liver (Fig. 4G), and decreased in the feces (Fig. 4H). These data demonstrate that hepatic FOXA3 is a positive regulator of macrophage cholesterol efflux and RCT.

Apoa1 is a direct target gene of FOXA3

The data of Figs. 2–4 suggest that ApoA-I may play a key role in FOXA3-mediated regulation of plasma HDL-c levels and RCT. Therefore, we explored whether and how FOXA3 regulates ApoA-I expression. Over-expression of FOXA3 induced *Apoa1* mRNA levels by 2 fold in primary hepatocytes (Fig. 5A). In contrast, knockdown of *Foxa3* in primary hepatocytes by adenoviruses, which did not show significant toxicity, reduced *Apoa1* mRNA levels by >50% (Supplementary Fig. IVA **and** IVB). In addition, we did pulse-chase studies in primary hepatocytes. The data show that over-expression of FOXA3 significantly increased newly synthesized [^{3}H]ApoA-I levels by 88% in hepatocytes and by 50% in culture media after 2 h of chasing (Fig. 5B). These data suggest that *Apoa1* may be a direct downstream target gene of FOXA3.

Furthermore, our transient transfection studies showed that FOXA3 over-expression induced *Apoa1* promoter activity by >2 fold in HepG2 cells (Fig. 5C). FOXA3 is shown to bind to the consensus binding site TGTTTAC [21]. There are two candidate *Foxa3* binding sites

separated by 6 bp in the proximal promoters of mouse *Apoa1* or human *APOA1* genes (Fig. 5D). Interestingly, only simultaneous mutations of both candidate binding sites (Mut½) abolished the induction of the *Apoa1* promoter activity by FOXA3 (Fig. 5E). In chromatin immunoprecipitation (ChIP) assays, FOXA3 protein was found to bind to the proximal promoter of the *Apoa1* gene promoter when liver lysates isolated from mice infected with Ad-Empty or Ad-hFOXA3 were used (Fig. 5F). We then performed electrophoretic mobility shift assays (EMSAs) using 293A lysates over-expressing FOXA3. FOXA3 protein bound to the wild-type (WT) DNA oligo containing the two candidate FOXA3 binding sites (Fig. 5G, lanes 3 and 4). The binding was competed away by oligos containing WT, Mut1 or Mut2 sequences (Fig. 5G, lanes 5–10), but not by oligos containing Mut½ sequences (Fig. 5G, lanes 11 and 12). Finally, the FOXA3/DNA complex was supershifted in the presence of an FOXA3 antibody (Fig. 5G, lane 15). Thus, the data of Fig. 5 indicate that FOXA3 directly binds to the proximal promoter of the *Apoa1* gene to regulate gene transcription.

Over-expression or knockdown of hepatic FOXA3 does not affect liver proliferation in adult mice

A previous study suggests that FOXA3 may be a strong promoter of liver regeneration [56]. However, over-expression or knockdown of hepatic *Foxa3* in C57BL/6J mice did not regulate hepatocyte proliferation or hepatic mRNA levels of cyclin D1 (*Ccnd1*), cyclin E1 (*Ccne1*) or *Foxm1* (Supplementary Fig. VA–D), suggesting that FOXA3 does not regulate liver proliferation in adult mice.

Hepatic FOXA3 regulates plasma HDL-c levels and Apoa1 expression in female mice

The above studies were performed in male C57BL/6J mice. To determine whether FOXA3 has a similar effect in female mice, we injected female C57BL/6J mice with Ad-FOXA3, Ad-shFoxa3 and their control adenoviruses. Over-expression of hepatic FOXA3 increased plasma HDL-c levels but had no effect on plasma levels of VLDL/LDL-c, triglyceride (TG) or glucose (Supplementary Fig. VIA **and** VIB). Over-expression of FOXA3 also induced hepatic *Apoa1*, *Apom*, *Lcat* and *Pon1* mRNA levels, but repressed hepatic *Saa1*, *Saa2* and *Saa3* mRNA levels (Supplementary Fig. VIC). In addition, hepatic FOXA3 over-expression did not affect intestinal *Apoa1* expression (Supplementary Fig. VID).

When hepatic *Foxa3* expression was deficient, plasma HDL-c levels were decreased, accompanied by unchanged plasma levels of VLDL/LDL-c, TG or glucose (Supplementary Fig. VIIA **and** VIIB). Hepatic *Foxa3* deficiency also led to a reduction in hepatic *Apoa1 mRNA levels* and an induction in hepatic *Saa1*, *Saa2*, *Saa3*, *Tnfα* and *Il6* expression (Supplementary Fig. VIIC). There was no change in intestinal *Apoa1* mRNA levels when hepatic *Foxa3* was deficient (Supplementary Fig. VIID).

AAV8-mediated expression of human FOXA3 induces ApoA-I expression and protects against diet-induced atherosclerosis in *Apoe*$^{-/-}$ mice

The findings that hepatic FOXA3 stimulates macrophage cholesterol efflux and RCT (Fig. 4) led us to investigate whether FOXA3 regulates the development of atherosclerosis. We therefore generated an adeno-associated virus serotype 8 (AAV8) expressing human FOXA3 under the control of an albumin promoter (AAV8-ALB-hFOXA3) and a control AAV

(AAV8-ALB-Null). These AAVs were injected into *Apoe*$^{-/-}$ mice, which were then fed a Western diet for 3 months. Over-expression of FOXA3 in hepatocytes reduced body fat by 30% (Supplementary Fig. VIIIA), and increased hepatic FOXA3 and ApoA-I protein levels by 1.9 fold and 4.7 fold, respectively (Fig. 6A and 6B). Plasma HDL-c levels were increased by 161% (Fig. 6C) whereas plasma levels of VLDL/LDL-c (Fig. 6D), total cholesterol, TG, glucose, ALT (P=0.06), AST, cortisol or testosterone were unchanged (Supplementary Fig. VIIIB–G). FPLC analysis of plasma lipoprotein profile showed that plasma HDL-c level was increased (Fig. 6E) whereas plasma TG lipoprotein profile was unchanged (Fig. 6F). Moreover, over-expression of FOXA3 significantly induced hepatic *Pon1* and *Apom* expression (Supplementary Fig. VIIIH).

En face analysis of aortas showed that over-expression of hepatocyte FOXA3 reduced aortic lesion size by 44% (Fig. 7A–C). In addition, over-expression of FOXA3 reduced atherosclerotic lesions by 37% (Fig. 7D and 7E), and macrophage infiltration by 29% (Fig. 7F and 7G) in aortic roots. The reduced macrophage infiltration is consistent with a role of ApoA-I in inhibiting monocyte activation and recruitment [57–60]. Thus, over-expression of FOXA3 in hepatocytes protects against diet-induced atherosclerosis in *Apoe*$^{-/-}$ mice.

Discussion

So far, the role of FOXA3 in lipid or lipoprotein metabolism is completely unknown. In this report, we demonstrate for the first time that hepatic FOXA3 induces ApoA-I expression and RCT, and inhibits the development of atherosclerosis. Thus, our current studies have revealed an important function of FOXA3 in lipid metabolism.

ApoA-I is the major apolipoprotein in HDL and plays a key role in HDL biogenesis and RCT. Increased plasma ApoA-I levels promote RCT and inhibit atherogenesis [8, 9, 54] whereas ApoA-I deficiency has opposite effects [10, 55]. Consistent with these findings, we show that hepatic FOXA3 regulates ApoA-I expression and the development of atherosclerosis. In addition, FOXA3 also regulates other genes involved in HDL biogenesis, such as ApoM and LCAT, which may also contribute to FOXA3-mediated regulation of RCT and atherosclerosis.

In addition to its well-known function in regulating cholesterol efflux, ApoA-I may also inhibit inflammation by inhibiting monocyte activation/recruitment via a mechanism involving cholesterol depletion [57–60] and by augmenting the effectiveness of the responsiveness of regulatory T (Treg) cells in lymph node [61]. During atherogenesis, Treg cells, which contribute to the anti-inflammatory response, are converted to pro-atherogenic T follicular helper (Tfh) cells [62]. Injection of lipid-free ApoA-I into *Ldlr*$^{-/-}$ mice reduces lipid and immune cell accumulation within the aortic root by systemically reducing microdomain cholesterol content in immune cells [11–13]. In *Apoe*$^{-/-}$ mice, lipid-free ApoA-I reduces intracellular cholesterol levels in Treg cells and prevents their conversion into Tfh cells [62]. Thus, FOXA3 may also regulate Treg cell population via ApoA-I to inhibit immune cell infiltration.

In addition to regulating RCT, HDL also has an anti-inflammatory effect. PON1 is associated with HDL and is partly responsible for HDL's atheroprotective properties, such as inhibition of LDL oxidation [16]. SAAs are also associated with HDL and can impair HDL's anti-inflammatory function [19]. PON1 and SAAs are shown to protect against [16] or promote [19] atherogenesis, respectively. Our data show that FOXA3 induces PON1 but inhibits SAAs, suggesting that FOXA3 may also play a role in conferring the anti-inflammatory property of HDL, which will be investigated in the future.

Although FOXA3 regulates the hepatic expression of *Pepck*, *Glut2* and *Cyp2c*, over-expression or knockdown of hepatic FOXA3 does not affect plasma glucose levels, suggesting that regulation of PEPCK or Glut2 by FOXA3 does not contribute to FOXA3's athero-protective effect. Human CYP2C8 and CYP2C9 are abundant in endothelial cells and are two of the main epoxygenases which convert arachidonic acid to epoxyeicosatrienoic acids (EETs) [63]. EETs have protective effects on human cardiovascular system [63]. However, mice have over 14 *Cyp2c* genes, and the mouse orthologs of human CYP2C8/9 are unclear [64]. In the current study, the changes in *Cyp2c* genes are limited to the liver, suggesting that *Cyp2c* genes may not have a major impact on FOXA3's anti-atherogenic effect.

A previous study shows that *Foxa3*$^{-/-}$ mice have reduced epididymal fat depot upon fed a high fat diet [34]. This observation is consistent with a role of FOXA3 in promoting adipocyte differentiation [34]. Interestingly, we show that hepatocyte-specific over-expression of FOXA3 in *Apoe*$^{-/-}$ mice protects against diet-induced obesity. Nonetheless, the reduction in obesity is associated with unchanged plasma triglyceride or VLDL/LDL-c levels, suggesting that the change in obesity is less likely to contribute to resistance to diet-induced atherogenesis. Thus, FOXA3 in different cell types/tissues may differentially regulate adipogenesis and energy metabolism. In humans, single-nucleotide polymorphism rs2866870 of FOXA3 is significantly associated with greater body mass index and lean body mass [65], and two missense mutations cause adipogenic function for FOXA3 [65]. Since FOXA3 is important for regulating adipogenesis, understanding how hepatocyte FOXA3 controls energy metabolism is one of our future directions.

The regulation of FOXA3 expression has been largely unknown. Zhao *et al.* show that *Foxa3* is significantly reduced in Leydig cells of diabetic mice, which may be partly responsible for reduced androgen production in these mice [66]. We find that hepatic FOXA3 expression is reduced in HFD-fed or diabetic mice and NASH patients. However, we do not see any change in plasma testosterone levels in our mouse models, which may be explained by the fact that FOXA3 expression is limited to the liver in this study. We further show that the reduced hepatic FOXA3 expression may result from elevated levels of free fatty acids. Other factors, such as microRNAs, are also induced under metabolic stress [35]. One of our future directions will determine how hepatic FOXA3 is repressed in obesity, diabetes or NAFLD.

The FoxO subfamily members FoxO1, FoxO3 and FoxO4 play an important role in insulin-regulated gene transcription [67]. Liver-specific knockout of *FoxO1/¾* leads to increased HDL-C levels and decreased SR-BI expression and HDL uptake [68]. Interestingly, FOXA3 up-regulates *FoxO1* and *FoxO4* expression but does not affect SR-BI expression. FOXA2 is also shown to regulate HDL levels via ApoM [69]. However, FOXA3 does not affect FOXA2

expression. Thus, FOXA3 regulates plasma HDL levels independent of regulation of FoxO1/¾ or FOXA2.

In summary, we have demonstrated that hepatic FOXA3 plays an important role in regulating ApoA-I expression, macrophage cholesterol efflux and RCT. We also show that AAV8-mediated over-expression of FOXA3 in hepatocytes protects against the development of atherosclerosis. Since hepatic FOXA3 expression is reduced under metabolic stress, our data suggest that hepatic FOXA3 may be a target for treatment of atherosclerosis.

Supplementary Material

Refer to Web version on PubMed Central for supplementary material.

Acknowledgements

b) **Sources of Funding.** This study was supported by grants from National Institutes of Health (R01HL103227 to L.Y and Y.Z., R01HL142086 to Y.Z., and R01DK118805 to Y.Z.).

Non-standard Abbreviations

Alb	Albumin
FOXA3	Forkhead box A3
HDL-c	HDL cholesterol
HFD	High fat diet
NASH	Non-alcoholic steatohepatitis
PON1	Paraoxonase 1
RCT	Reverse cholesterol transport
SAA	Serum amyloid A

References

1. Yamashita S, Sakai N, Hirano K, Ishigami M, Maruyama T, Nakajima N, Matsuzawa Y. Roles of plasma lipid transfer proteins in reverse cholesterol transport. Front Biosci. 2001;6:D366–387 [PubMed: 11229884]
2. Toth PP, Barter PJ, Rosenson RS, Boden WE, Chapman MJ, Cuchel M, D'Agostino RB Sr., Davidson MH, Davidson WS, Heinecke JW, Karas RH, Kontush A, Krauss RM, Miller M, Rader DJ. High-density lipoproteins: A consensus statement from the national lipid association. J Clin Lipidol. 2013;7:484–525 [PubMed: 24079290]
3. Lee-Rueckert M, Escola-Gil JC, Kovanen PT. Hdl functionality in reverse cholesterol transport--challenges in translating data emerging from mouse models to human disease. Biochim Biophys Acta. 2016;1861:566–583 [PubMed: 26968096]
4. Kosmas CE, Christodoulidis G, Cheng JW, Vittorio TJ, Lerakis S. High-density lipoprotein functionality in coronary artery disease. Am J Med Sci. 2014;347:504–508 [PubMed: 24603157]
5. Rubin EM, Krauss RM, Spangler EA, Verstuyft JG, Clift SM. Inhibition of early atherogenesis in transgenic mice by human apolipoprotein ai. Nature. 1991;353:265–267 [PubMed: 1910153]

6. Liu AC, Lawn RM, Verstuyft JG, Rubin EM. Human apolipoprotein a-i prevents atherosclerosis associated with apolipoprotein[a] in transgenic mice. J Lipid Res. 1994;35:2263–2267 [PubMed: 7897323]
7. Plump AS, Scott CJ, Breslow JL. Human apolipoprotein a-i gene expression increases high density lipoprotein and suppresses atherosclerosis in the apolipoprotein e-deficient mouse. Proc Natl Acad Sci U S A. 1994;91:9607–9611 [PubMed: 7937814]
8. Zhang Y, Zanotti I, Reilly MP, Glick JM, Rothblat GH, Rader DJ. Overexpression of apolipoprotein a-i promotes reverse transport of cholesterol from macrophages to feces in vivo. Circulation. 2003;108:661–663 [PubMed: 12900335]
9. Navab M, Anantharamaiah GM, Hama S, Garber DW, Chaddha M, Hough G, Lallone R, Fogelman AM. Oral administration of an apo a-i mimetic peptide synthesized from d-amino acids dramatically reduces atherosclerosis in mice independent of plasma cholesterol. Circulation. 2002;105:290–292 [PubMed: 11804981]
10. Moore RE, Navab M, Millar JS, Zimetti F, Hama S, Rothblat GH, Rader DJ. Increased atherosclerosis in mice lacking apolipoprotein a-i attributable to both impaired reverse cholesterol transport and increased inflammation. Circ Res. 2005;97:763–771 [PubMed: 16151025]
11. Kaul S, Xu H, Zabalawi M, Maruko E, Fulp BE, Bluemn T, Brzoza-Lewis KL, Gerelus M, Weerasekera R, Kallinger R, James R, Zhang YS, Thomas MJ, Sorci-Thomas MG. Lipid-free apolipoprotein a-i reduces progression of atherosclerosis by mobilizing microdomain cholesterol and attenuating the number of cd131 expressing cells: Monitoring cholesterol homeostasis using the cellular ester to total cholesterol ratio. J Am Heart Assoc. 2016;5
12. Madenspacher JH, Azzam KM, Gong W, Gowdy KM, Vitek MP, Laskowitz DT, Remaley AT, Wang JM, Fessler MB. Apolipoproteins and apolipoprotein mimetic peptides modulate phagocyte trafficking through chemotactic activity. J Biol Chem. 2012;287:43730–43740 [PubMed: 23118226]
13. Murphy AJ, Woollard KJ, Suhartoyo A, Stirzaker RA, Shaw J, Sviridov D, Chin-Dusting JP. Neutrophil activation is attenuated by high-density lipoprotein and apolipoprotein a-i in in vitro and in vivo models of inflammation. Arterioscler Thromb Vasc Biol. 2011;31:1333–1341 [PubMed: 21474825]
14. Wolfrum C, Poy MN, Stoffel M. Apolipoprotein m is required for prebeta-hdl formation and cholesterol efflux to hdl and protects against atherosclerosis. Nat Med. 2005;11:418–422 [PubMed: 15793583]
15. Barter PJ, Nicholls S, Rye KA, Anantharamaiah GM, Navab M, Fogelman AM. Antiinflammatory properties of hdl. Circ Res. 2004;95:764–772 [PubMed: 15486323]
16. Aviram M, Vaya J. Paraoxonase 1 activities, regulation, and interactions with atherosclerotic lesion. Curr Opin Lipidol. 2013;24:339–344 [PubMed: 23508039]
17. Banka CL, Yuan T, de Beer MC, Kindy M, Curtiss LK, de Beer FC. Serum amyloid a (saa): Influence on hdl-mediated cellular cholesterol efflux. J Lipid Res. 1995;36:1058–1065 [PubMed: 7658153]
18. Nishida E, Aino M, Kobayashi SI, Okada K, Ohno T, Kikuchi T, Hayashi JI, Yamamoto G, Hasegawa Y, Mitani A. Serum amyloid a promotes e-selectin expression via toll-like receptor 2 in human aortic endothelial cells. Mediators Inflamm. 2016;2016:7150509 [PubMed: 27799725]
19. Getz GS, Krishack PA, Reardon CA. Serum amyloid a and atherosclerosis. Curr Opin Lipidol. 2016;27:531–535 [PubMed: 27579547]
20. Van Lenten BJ, Hama SY, de Beer FC, Stafforini DM, McIntyre TM, Prescott SM, La Du BN, Fogelman AM, Navab M. Anti-inflammatory hdl becomes pro-inflammatory during the acute phase response. Loss of protective effect of hdl against ldl oxidation in aortic wall cell cocultures. J Clin Invest. 1995;96:2758–2767 [PubMed: 8675645]
21. Motallebipour M, Ameur A, Reddy Bysani MS, Patra K, Wallerman O, Mangion J, Barker MA, McKernan KJ, Komorowski J, Wadelius C. Differential binding and co-binding pattern of foxa1 and foxa3 and their relation to h3k4me3 in hepg2 cells revealed by chip-seq. Genome Biol. 2009;10:R129 [PubMed: 19919681]

22. Iwafuchi-Doi M, Donahue G, Kakumanu A, Watts JA, Mahony S, Pugh BF, Lee D, Kaestner KH, Zaret KS. The pioneer transcription factor foxa maintains an accessible nucleosome configuration at enhancers for tissue-specific gene activation. Mol Cell. 2016;62:79–91 [PubMed: 27058788]
23. Nakamori D, Akamine H, Takayama K, Sakurai F, Mizuguchi H. Direct conversion of human fibroblasts into hepatocyte-like cells by atf5, prox1, foxa2, foxa3, and hnf4a transduction. Sci Rep. 2017;7:16675 [PubMed: 29192290]
24. Huang P, He Z, Ji S, Sun H, Xiang D, Liu C, Hu Y, Wang X, Hui L. Induction of functional hepatocyte-like cells from mouse fibroblasts by defined factors. Nature. 2011;475:386–389 [PubMed: 21562492]
25. Huang P, Zhang L, Gao Y, et al. Direct reprogramming of human fibroblasts to functional and expandable hepatocytes. Cell Stem Cell. 2014;14:370–384 [PubMed: 24582927]
26. Yu B, He ZY, You P, et al. Reprogramming fibroblasts into bipotential hepatic stem cells by defined factors. Cell Stem Cell. 2013;13:328–340 [PubMed: 23871605]
27. Behr R, Sackett SD, Bochkis IM, Le PP, Kaestner KH. Impaired male fertility and atrophy of seminiferous tubules caused by haploinsufficiency for foxa3. Dev Biol. 2007;306:636–645 [PubMed: 17488644]
28. Garon G, Bergeron F, Brousseau C, Robert NM, Tremblay JJ. Foxa3 is expressed in multiple cell lineages in the mouse testis and regulates pdgfra expression in leydig cells. Endocrinology. 2017;158:1886–1897 [PubMed: 28379539]
29. O'Brien RM, Noisin EL, Suwanichkul A, Yamasaki T, Lucas PC, Wang JC, Powell DR, Granner DK. Hepatic nuclear factor 3- and hormone-regulated expression of the phosphoenolpyruvate carboxykinase and insulin-like growth factor-binding protein 1 genes. Mol Cell Biol. 1995;15:1747–1758 [PubMed: 7532283]
30. Lin B, Morris DW, Chou JY. The role of hnf1alpha, hnf3gamma, and cyclic amp in glucose-6-phosphatase gene activation. Biochemistry. 1997;36:14096–14106 [PubMed: 9369482]
31. Shen W, Scearce LM, Brestelli JE, Sund NJ, Kaestner KH. Foxa3 (hepatocyte nuclear factor 3gamma) is required for the regulation of hepatic glut2 expression and the maintenance of glucose homeostasis during a prolonged fast. J Biol Chem. 2001;276:42812–42817 [PubMed: 11546810]
32. Ma X, Xu L, Mueller E. Forkhead box a3 mediates glucocorticoid receptor function in adipose tissue. Proc Natl Acad Sci U S A. 2016;113:3377–3382 [PubMed: 26957608]
33. Ma X, Xu L, Gavrilova O, Mueller E. Role of forkhead box protein a3 in age-associated metabolic decline. Proc Natl Acad Sci U S A. 2014;111:14289–14294 [PubMed: 25225406]
34. Xu L, Panel V, Ma X, Du C, Hugendubler L, Gavrilova O, Liu A, McLaughlin T, Kaestner KH, Mueller E. The winged helix transcription factor foxa3 regulates adipocyte differentiation and depot-selective fat tissue expansion. Mol Cell Biol. 2013;33:3392–3399 [PubMed: 23798556]
35. Xu Y, Zalzala M, Xu J, Li Y, Yin L, Zhang Y. A metabolic stress-inducible mir-34a-hnf4alpha pathway regulates lipid and lipoprotein metabolism. Nat Commun. 2015;6:7466 [PubMed: 26100857]
36. Zhang Y, Lee FY, Barrera G, Lee H, Vales C, Gonzalez FJ, Willson TM, Edwards PA. Activation of the nuclear receptor fxr improves hyperglycemia and hyperlipidemia in diabetic mice. Proc Natl Acad Sci U S A. 2006;103:1006–1011 [PubMed: 16410358]
37. Zhang Y, Yin L, Hillgartner FB. Srebp-1 integrates the actions of thyroid hormone, insulin, camp, and medium-chain fatty acids on accalpha transcription in hepatocytes. J Lipid Res. 2003;44:356–368 [PubMed: 12576518]
38. Xu J, Li Y, Chen W, Xu Y, Yin L, Ge X, Jadhav K, Adorini L, Zhang Y. Hepatic carboxylesterase 1 is essential for both normal and farnesoid x-receptor-controlled lipid homeostasis. Hepatology. 2014;59:1761–1771 [PubMed: 24038130]
39. Li Y, Zalzala M, Jadhav K, Xu Y, Kasumov T, Yin L, Zhang Y. Carboxylesterase 2 prevents liver steatosis by modulating lipolysis, endoplasmic reticulum stress, and lipogenesis and is regulated by hepatocyte nuclear factor 4 alpha in mice. Hepatology. 2016;63:1860–1874 [PubMed: 26806650]
40. Zhang Y, Castellani LW, Sinal CJ, Gonzalez FJ, Edwards PA. Peroxisome proliferator-activated receptor-gamma coactivator 1alpha (pgc-1alpha) regulates triglyceride metabolism by activation of the nuclear receptor fxr. Genes Dev. 2004;18:157–169 [PubMed: 14729567]

41. Liao D, Tan H, Hui R, Li Z, Jiang X, Gaubatz J, Yang F, Durante W, Chan L, Schafer AI, Pownall HJ, Yang X, Wang H. Hyperhomocysteinemia decreases circulating high-density lipoprotein by inhibiting apolipoprotein a-i protein synthesis and enhancing hdl cholesterol clearance. Circ Res. 2006;99:598–606 [PubMed: 16931800]
42. Yin L, Ma H, Ge X, Edwards PA, Zhang Y. Hepatic hepatocyte nuclear factor 4alpha is essential for maintaining triglyceride and cholesterol homeostasis. Arterioscler Thromb Vasc Biol. 2011;31:328–336 [PubMed: 21071704]
43. Naik SU, Wang X, Da Silva JS, Jaye M, Macphee CH, Reilly MP, Billheimer JT, Rothblat GH, Rader DJ. Pharmacological activation of liver x receptors promotes reverse cholesterol transport in vivo. Circulation. 2006;113:90–97 [PubMed: 16365197]
44. Xu Y, Li F, Zalzala M, Xu J, Gonzalez FJ, Adorini L, Lee YK, Yin L, Zhang Y. Fxr activation increases reverse cholesterol transport by modulating bile acid composition and cholesterol absorption. Hepatology. 2016;64:1072–1085 [PubMed: 27359351]
45. Daugherty A, Tall AR, Daemen M, Falk E, Fisher EA, Garcia-Cardena G, Lusis AJ, Owens AP 3rd, Rosenfeld ME, Virmani R, American Heart Association Council on Arteriosclerosis T, Vascular B, Council on Basic Cardiovascular S. Recommendation on design, execution, and reporting of animal atherosclerosis studies: A scientific statement from the american heart association. Arterioscler Thromb Vasc Biol. 2017;37:e131–e157 [PubMed: 28729366]
46. Bourassa PA, Milos PM, Gaynor BJ, Breslow JL, Aiello RJ. Estrogen reduces atherosclerotic lesion development in apolipoprotein e-deficient mice. Proc Natl Acad Sci U S A. 1996;93:10022–10027 [PubMed: 8816744]
47. Zhang Y, Wang X, Vales C, Lee FY, Lee H, Lusis AJ, Edwards PA. Fxr deficiency causes reduced atherosclerosis in ldlr−/− mice. Arterioscler Thromb Vasc Biol. 2006;26:2316–2321 [PubMed: 16825595]
48. Liu J, Yang P, Zuo G, He S, Tan W, Zhang X, Su C, Zhao L, Wei L, Chen Y, Ruan X, Chen Y. Long-chain fatty acid activates hepatocytes through cd36 mediated oxidative stress. Lipids Health Dis. 2018;17:153 [PubMed: 30016988]
49. Hayakawa J, Wang M, Wang C, Han RH, Jiang ZY, Han X. Lipidomic analysis reveals significant lipogenesis and accumulation of lipotoxic components in ob/ob mouse organs. Prostaglandins Leukot Essent Fatty Acids. 2018;136:161–169 [PubMed: 28110829]
50. Eisinger K, Krautbauer S, Hebel T, Schmitz G, Aslanidis C, Liebisch G, Buechler C. Lipidomic analysis of the liver from high-fat diet induced obese mice identifies changes in multiple lipid classes. Exp Mol Pathol. 2014;97:37–43 [PubMed: 24830603]
51. Donnelly KL, Smith CI, Schwarzenberg SJ, Jessurun J, Boldt MD, Parks EJ. Sources of fatty acids stored in liver and secreted via lipoproteins in patients with nonalcoholic fatty liver disease. J Clin Invest. 2005;115:1343–1351 [PubMed: 15864352]
52. Lee JJ, Lambert JE, Hovhannisyan Y, Ramos-Roman MA, Trombold JR, Wagner DA, Parks EJ. Palmitoleic acid is elevated in fatty liver disease and reflects hepatic lipogenesis. Am J Clin Nutr. 2015;101:34–43 [PubMed: 25527748]
53. Bort R, Gomez-Lechon MJ, Castell JV, Jover R. Role of hepatocyte nuclear factor 3 gamma in the expression of human cyp2c genes. Arch Biochem Biophys. 2004;426:63–72 [PubMed: 15130783]
54. Lebherz C, Sanmiguel J, Wilson JM, Rader DJ. Gene transfer of wild-type apoa-i and apoa-i milano reduce atherosclerosis to a similar extent. Cardiovasc Diabetol. 2007;6:15 [PubMed: 17475009]
55. Moore RE, Kawashiri MA, Kitajima K, Secreto A, Millar JS, Pratico D, Rader DJ. Apolipoprotein a-i deficiency results in markedly increased atherosclerosis in mice lacking the ldl receptor. Arterioscler Thromb Vasc Biol. 2003;23:1914–1920 [PubMed: 12933536]
56. Wangensteen KJ, Zhang S, Greenbaum LE, Kaestner KH. A genetic screen reveals foxa3 and tnfr1 as key regulators of liver repopulation. Genes Dev. 2015;29:904–909 [PubMed: 25934503]
57. Murphy AJ, Woollard KJ, Hoang A, Mukhamedova N, Stirzaker RA, McCormick SP, Remaley AT, Sviridov D, Chin-Dusting J. High-density lipoprotein reduces the human monocyte inflammatory response. Arterioscler Thromb Vasc Biol. 2008;28:2071–2077 [PubMed: 18617650]

58. Diederich W, Orso E, Drobnik W, Schmitz G. Apolipoprotein ai and hdl(3) inhibit spreading of primary human monocytes through a mechanism that involves cholesterol depletion and regulation of cdc42. Atherosclerosis. 2001;159:313–324 [PubMed: 11730811]
59. Iqbal AJ, Barrett TJ, Taylor L, McNeill E, Manmadhan A, Recio C, Carmineri A, Brodermann MH, White GE, Cooper D, DiDonato JA, Zamanian-Daryoush M, Hazen SL, Channon KM, Greaves DR, Fisher EA. Acute exposure to apolipoprotein a1 inhibits macrophage chemotaxis in vitro and monocyte recruitment in vivo. Elife. 2016;5
60. Smythies LE, White CR, Maheshwari A, Palgunachari MN, Anantharamaiah GM, Chaddha M, Kurundkar AR, Datta G. Apolipoprotein a-i mimetic 4f alters the function of human monocyte-derived macrophages. Am J Physiol Cell Physiol. 2010;298:C1538–1548 [PubMed: 20219948]
61. Wilhelm AJ, Zabalawi M, Owen JS, Shah D, Grayson JM, Major AS, Bhat S, Gibbs DP Jr., Thomas MJ, Sorci-Thomas MG. Apolipoprotein a-i modulates regulatory t cells in autoimmune ldlr−/−, apoa-i−/− mice. J Biol Chem. 2010;285:36158–36169 [PubMed: 20833724]
62. Gaddis DE, Padgett LE, Wu R, McSkimming C, Romines V, Taylor AM, McNamara CA, Kronenberg M, Crotty S, Thomas MJ, Sorci-Thomas MG, Hedrick CC. Apolipoprotein ai prevents regulatory to follicular helper t cell switching during atherosclerosis. Nat Commun. 2018;9:1095 [PubMed: 29545616]
63. Shahabi P, Siest G, Visvikis-siest S. Influence of inflammation on cardiovascular protective effects of cytochrome p450 epoxygenase-derived epoxyeicosatrienoic acids. Drug Metab Rev. 2014;46:33–56 [PubMed: 24040964]
64. Scheer N, Kapelyukh Y, Chatham L, Rode A, Buechel S, Wolf CR. Generation and characterization of novel cytochrome p450 cyp2c gene cluster knockout and cyp2c9 humanized mouse lines. Mol Pharmacol. 2012;82:1022–1029 [PubMed: 22918969]
65. Adler-Wailes DC, Alberobello AT, Ma X, Hugendubler L, Stern EA, Mou Z, Han JC, Kim PW, Sumner AE, Yanovski JA, Mueller E. Analysis of variants and mutations in the human winged helix foxa3 gene and associations with metabolic traits. Int J Obes (Lond). 2015;39:888–892 [PubMed: 25672906]
66. Zhao Y, Li HX, Wang K, Yan BY, Li W. Regulation of testicular steroidogenesis by foxa3 via transcriptional modulation of eralpha signaling in type 2 diabetes mellitus (t2dm). Biochem Biophys Res Commun. 2017;490:786–793 [PubMed: 28645613]
67. Accili D, Arden KC. Foxos at the crossroads of cellular metabolism, differentiation, and transformation. Cell. 2004;117:421–426 [PubMed: 15137936]
68. Lee SX, Heine M, Schlein C, Ramakrishnan R, Liu J, Belnavis G, Haimi I, Fischer AW, Ginsberg HN, Heeren J, Rinninger F, Haeusler RA. Foxo transcription factors are required for hepatic hdl cholesterol clearance. J Clin Invest. 2018;128:1615–1626 [PubMed: 29408809]
69. Wolfrum C, Howell JJ, Ndungo E, Stoffel M. Foxa2 activity increases plasma high density lipoprotein levels by regulating apolipoprotein m. J Biol Chem. 2008;283:16940–16949 [PubMed: 18381283]

Highlights

- Hepatic FOXA3 expression is reduced in diabetic or high fat diet-fed mice and NASH patients
- Hepatic FOXA3 is a positive regulator of ApoA-I expression and plasma HDL-c levels
- Hepatic FOXA3 regulates macrophage cholesterol efflux and reverse cholesterol transport
- ApoA-I is a direct target of FOXA3
- AAV8-mediated over-expression of FOXA3 in hepatocytes protects against the development of atherosclerosis in *Apoe*$^{-/-}$ mice

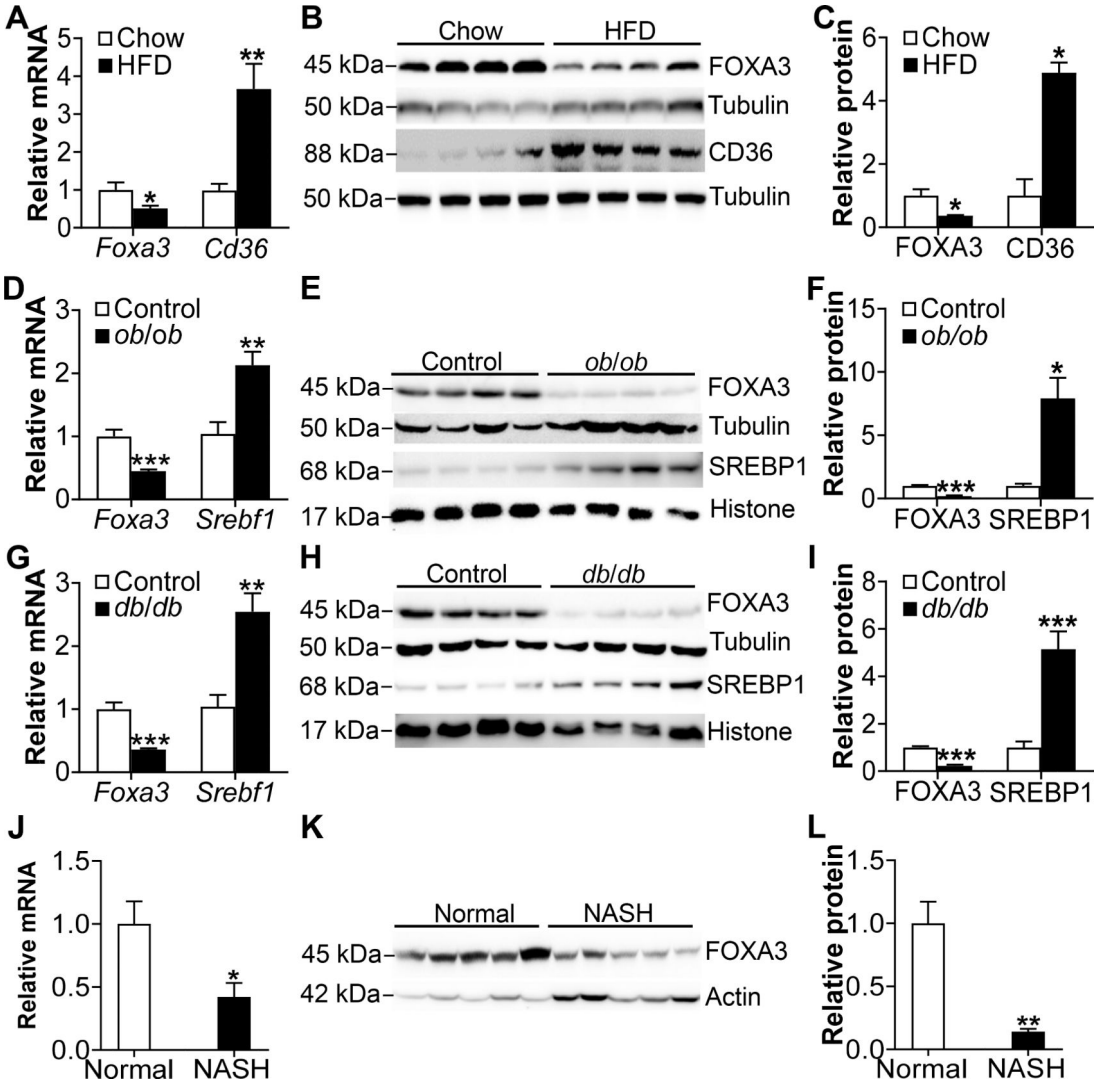

Figure 1. Hepatic FOXA3 is reduced in HFD-fed or diabetic mice as well as NASH patients.

A-C, Hepatic mRNA levels in chow or high fat diet (HFD)-fed mice were quantified by qRT-PCR (**A**) (n=6 per group). Protein levels were determined by Western blotting (**B**) and then quantified (**C**). **D-F**, Hepatic levels of mRNA (**D**) or proteins (**E**, **F**) were determined in *ob/ob or* lean (control) mice (n=6 per group). **G-I,** Hepatic levels of mRNA (**G**) or proteins (**H**, **I**) were determined in *db/db or* lean (control) mice (n=6 per group). **J-K**, Hepatic levels of mRNA (**J**) or proteins (**K**, **L**) were determined in normal individuals or NASH patients (n=8 per group). *Cd36* and *Srebf1* serve as positive controls in **A** and **D** or **G**, respectively. * $P<0.05$, ** $P<0.01$, *** $P<0.001$

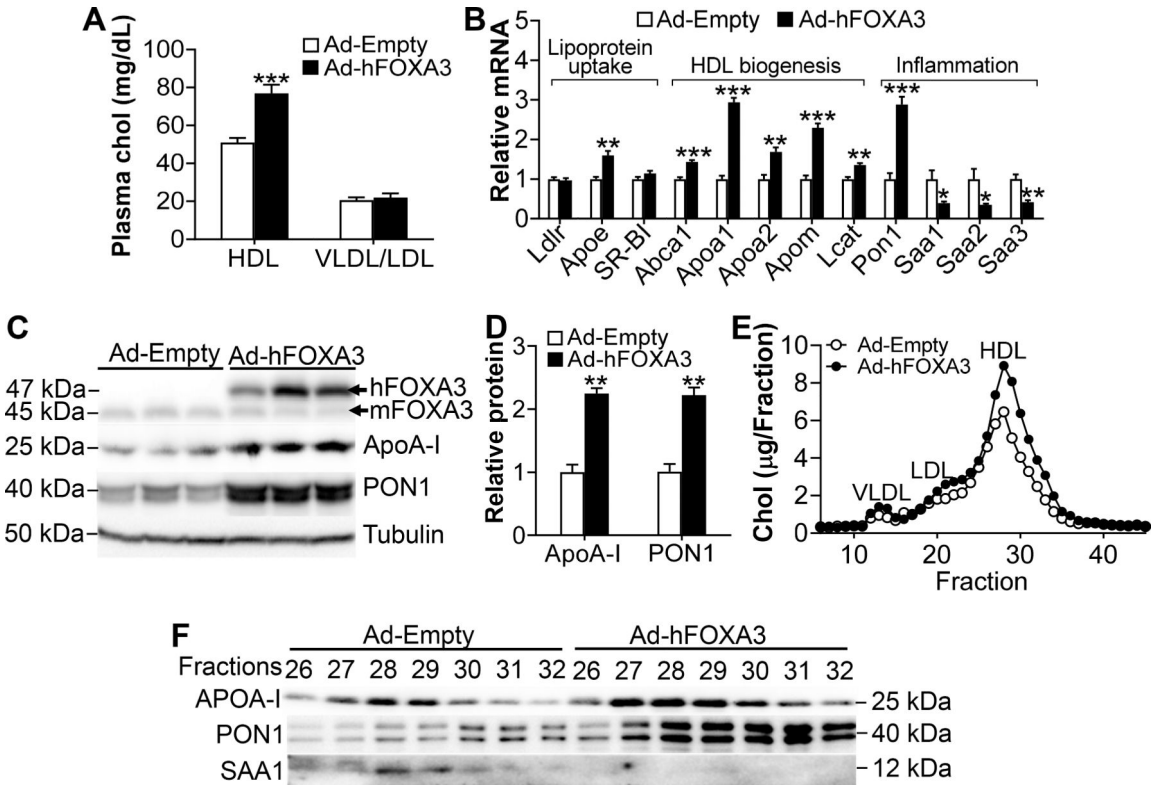

Figure 2. Hepatic over-expression of FOXA3 increases HDL-c and ApoA-I levels.

C57BL/6J mice were i.v. injected with adenoviruses expressing human FOXA3 (Ad-hFOXA3) or control adenoviruses (Ad-Empty) (n=8 per group). After 7 days, mice were sacrificed. **A**, Plasma HDL-c and VLDL/LDL-c levels. **B**, Relative mRNA levels of hepatic genes involved in lipoprotein uptake, HDL biogenesis or inflammation. **C** and **D**, Hepatic protein levels were determined by Western blotting (**C**) and then quantified (**D**). **E**, FPLC analysis of plasma lipoprotein profile. **F**, Protein levels in individual HDL fractions were determined by Western blotting. * $P < 0.05$; ** $P < 0.01$; *** $P < 0.001$.

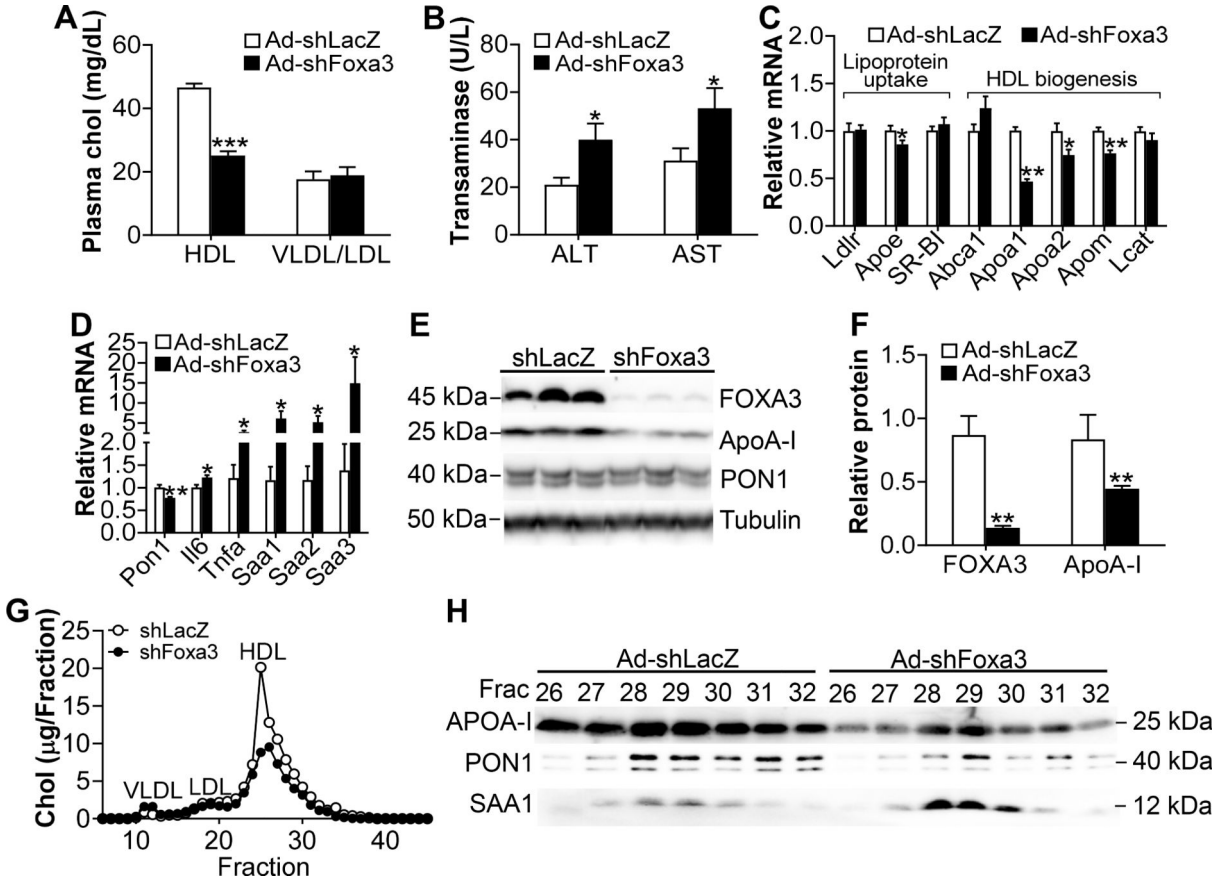

Figure 3. Knockdown of hepatic FOXA3 decreases HDL-c and ApoA-I levels.

C57BL/6J mice were i.v. injected with adenoviruses expressing shRNA against LacZ (Ad-shLacZ) or *Foxa3* (Ad-shFoxa3) (n=8 mice per group). Mice were sacrificed 7 days later. **A**, Plasma HDL-c and VLDL/LDL-c levels. **B**, Plasma ALT and AST level. **C** and **D**, Hepatic levels of genes involved in lipoprotein uptake or HDL biogenesis (**B**) or inflammation (**C**). **E** and **F**, Hepatic protein levels were determined by Western blotting (**E**) and then quantified (**F**). **G**, FPLC analysis of plasma lipoprotein profile. **H**, Protein levels in individual HDL fractions were determined by Western blotting. * $P < 0.05$. ** $P < 0.01$, *** $P < 0.001$

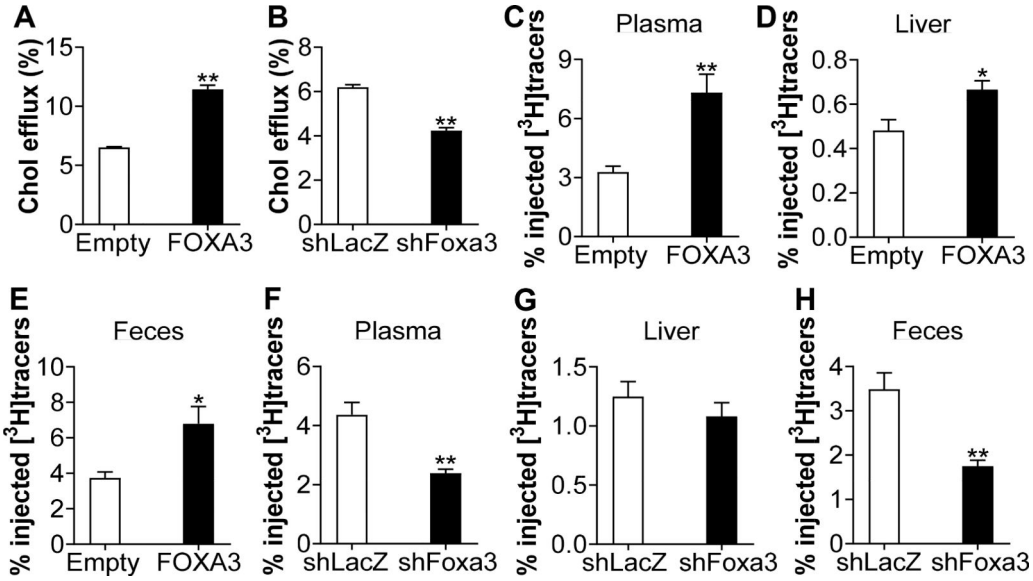

Figure 4. Hepatic FOXA3 regulates macrophage cholesterol efflux and reverse cholesterol transport.

C57BL/6J mice were i.v. injected with adenoviruses expressing FOXA3 or shRNA against *Foxa3* or their control adenoviruses. **A** and **B**, Cholesterol efflux was performed using ApoB-depleted plasma (n=6–7 per group). **C-E**, Macrophage reverse cholesterol transport was performed in mice injected with Ad-Empty or Ad-FOXA3. At 48 h, [^{3}H]tracers in the plasma (**C**), liver (**D**) or feces (**E**) were determined (n=7–8 per group). **F-H**, Macrophage reverse cholesterol transport was performed in mice injected with Ad-shLacZ or Ad-shFoxa3. At 48 h, [^{3}H]tracers in the plasma (**F**), liver (**G**) or feces (**H**) were determined (n=7–8 per group). * $P < 0.05$, ** $P < 0.01$, *** $P < 0.001$

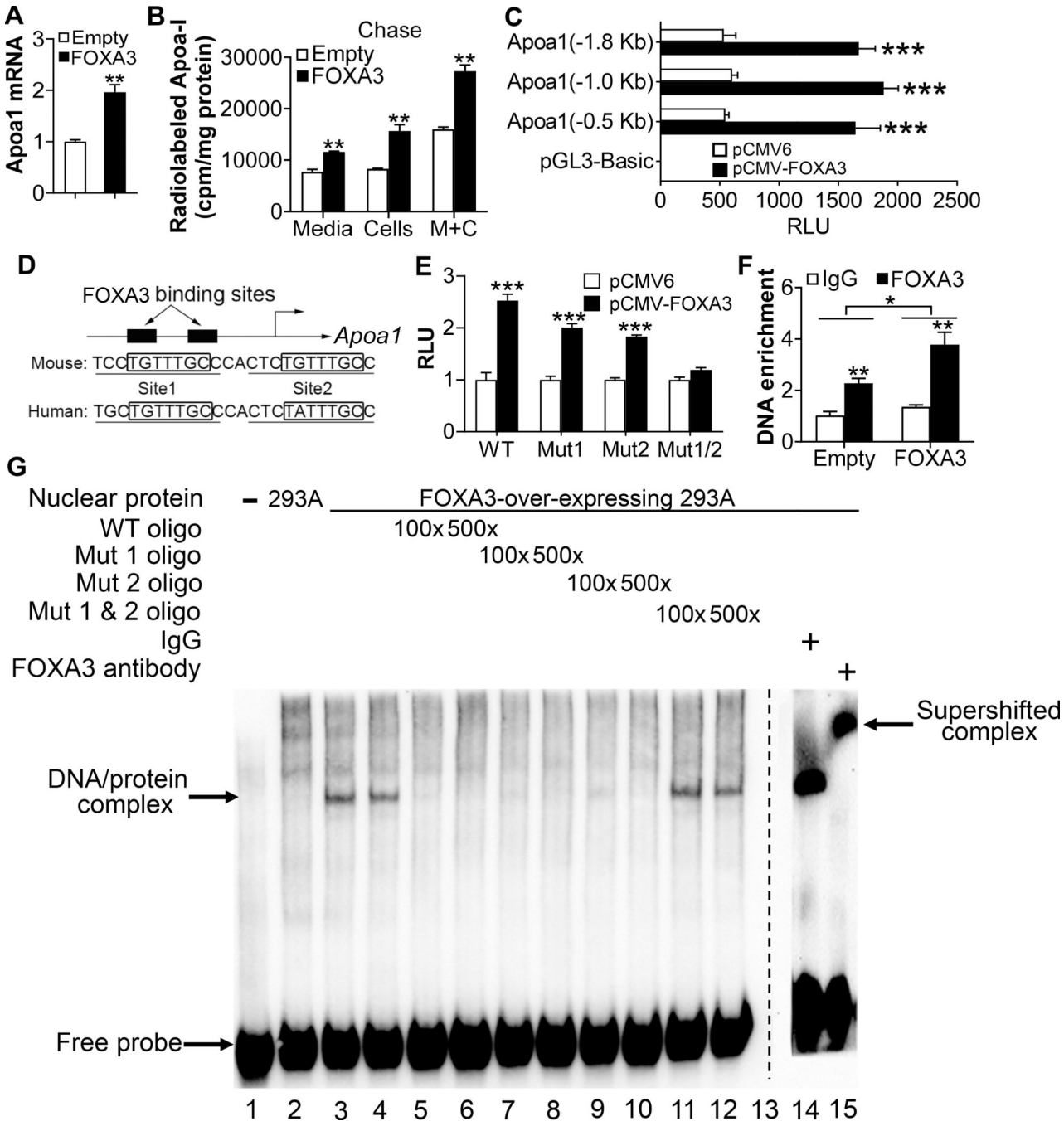

Figure 5. *Apoa1* is a direct target gene of FOXA3.

A, Mouse primary hepatocytes were infected with Ad-Empty or Ad-FOXA3 for 24 h. mRNA levels were determined by real-time qPCR (n=3). **B**, Pulse-chase analysis of ApoA-I synthesis. Mouse primary hepatocytes were infected with Ad-Empty or Ad-FOXA3 for 24 h, pulsed with [^{3}H]-Leucine for 2 h, and chased for 2 h. Radio-labeled ApoA-I in the media, cells and media plus cells (M+C) were determined. **C**, HepG2 cells were transfected with pGL3-basic or pGL3-Apoa1 luciferase-promoter constructs together with pCMV6 (control) or pCMV-FOXA3. After 36 h, relative luciferase units (RLU) were determined (n=5). **D**,

The *Apoa1* promoter has two putative FOXA3 binding sites. **E**, HepG2 cells were transfected with *Apoa1* luciferase-promoter constructs containing wild-type or mutant FOXA3 binding site(s). After 36 h, RLU was determined (n=6). **F**, ChIP assay was performed by incubating IgG or FOXA3 antibodies with liver extracts of mice infected with Ad-Empty or Ad-FOXA3 (n=4). **G**, EMSA was carried out using 293A cell lysates overexpressing FOXA3 in the presence of oligos containing wild-type (WT) or mutant FOXA3 binding sites. For the competing study, the addition of an FOXA3 antibody disrupted the interaction between wild-type oligo and FOXA3 protein * $P < 0.05$, ** $P < 0.01$, *** $P<0.001$

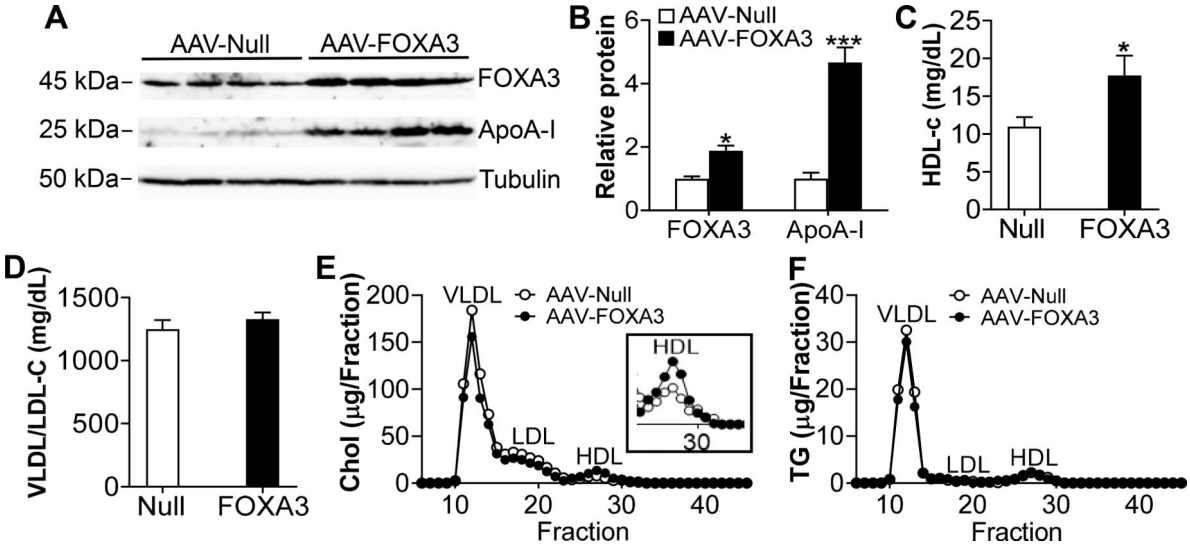

Figure 6. AAV-mediated over-expression of FOXA3 in hepatocytes induces ApoA-I expression and raises HDL-C levels in *Apoe*$^{-/-}$ mice.

Apoe$^{-/-}$ mice were i.v. injected with AAV8-ALB-Null or AAV8-ALB-FOXA3 and then fed a Western diet for 3 months (n=10–12 per group). **A** and **B**, Hepatic protein levels were analyzed by Western blotting (**A**) and then quantified (**B**). **C**, Plasma HDL-c levels. **D**, Plasma VLDL/LDL-c levels. **E** and **F**, FPLC analysis of plasma cholesterol (chol) (**E**) or TG (**F**) lipoprotein profiles. In the inlet of **E**, the HDL fraction is shown. * $P< 0.05$, ** $P< 0.01$, *** $P<0.001$.

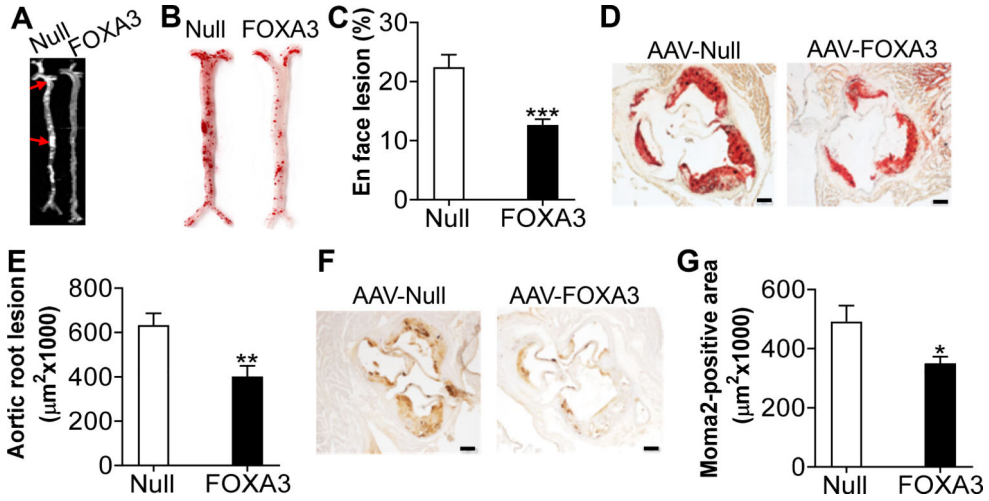

Figure 7. Hepatocyte-specific over-expression of FOXA3 attenuates the development of atherosclerosis.

Apoe$^{-/-}$ mice were i.v. injected with AAV8-ALB-Null or AAV8-ALB-FOXA3 and then fed a Western diet for 3 months (n=10–12 per group). **A**, Representative images of aortas. Red arrows point to lesions. **B**, Representative images of aortas stained by oil red O. **C**, *En face* lesion area (%) of aortas. **D**, Representative images of aortic roots stained by oil red O. **E**, Lesion size of aortic roots. **F** and **G**, Aortic roots were immunostained with an MOMA-2 antibody (**F**) and staining-positive areas were quantified (**G**). In **D** and **F**, scale bars stand for 200 μm. * $P< 0.05$, ** $P< 0.01$, *** $P< 0.001$